

Near-surface fluxes of cloud water evolve vertically

By A. S. KOWALSKI* and R. J. VONG
Oregon State University, USA

(Received 8 September 1997; revised 6 February 1999)

SUMMARY

Occult deposition to vegetation, via mechanical interception of wind-blown cloud water, can be a significant fraction of total ionic chemical deposition for some forests. Applying micrometeorological methods to the estimation of cloud water deposition requires particular consideration since cloud droplets are not conservative but are subject to material change (phase change); sedimentation also affects fluxes of droplets. The budget equation for liquid water (LW) in orographic cloud predicts that LW fluxes will diverge due to condensation during mean ascent. For hilltop measurements such as these, other factors can contribute to changes in the vertical flux with height above the surface.

Fluxes measured concurrently at two heights exhibit a persistent and significant divergence, while laterally separated measurements are found to agree. A LW budget equation is presented and simplified by scale analysis. Surface uptake is estimated by extrapolation of the measured fluxes. Estimated surface deposition is found to be substantially different from the flux measured at a reference height (10 m), often by a factor of two and occasionally with a different sign. This difference in estimated surface uptake extends to estimates of chemical as well as water deposition. The turbulent flux of LW is shown to be dependent on two criteria for describing 'steady-cloud' conditions, thus presumably minimizing the effects of entrainment. An often used model relating droplet deposition to the 'deposition velocity' for momentum is found to be inappropriate for application in complex terrain. Deposition of LW is estimated to range from 5 to 50 mg m⁻² s⁻¹ during the third field campaign of the Cloud and Aerosol CHEmistry Experiment (CACHE-3), with an average of 19 mg m⁻² s⁻¹ (nearly 2 mm per in-cloud day) in late summer at this Pacific coastal site in North America.

KEYWORDS: Cloud water Complex terrain Deposition Non-conservative Slinn model

1. INTRODUCTION

Describing surface fluxes from atmospheric measurements requires assumptions to be made about the variation in the flux with height. Prevailing methods in micrometeorology such as the Monin–Obukhov similarity theory (Wyngaard 1973) and the method of multiple resistances (Shuttleworth 1976) are established means of predicting fluxes of some conservative scalars to relatively simple surfaces. Now it is increasingly of interest to determine appropriate relationships for more common cases of land–atmosphere interaction which include non-conservative scalars and complex terrain. This paper presents a method of estimating deposition of cloud water, a non-conservative quantity in the atmosphere, from eddy correlation (EC) flux measurements over a hillside forest. The method derives from direct observations of a divergence in the surface-normal (vertical) cloud-water flux and yields appreciably different results from predictions made with the traditional 'constant flux layer' assumption.

Mechanical interception of wind-blown cloud water, termed occult precipitation because it is not measured by rain-gauges, is a significant pathway for hydrologic and acidic input to certain forests, usually in complex terrain. Decline of high-elevation forests in eastern North America has been attributed to the effects of acid deposition (NAPAP 1993). Occult deposition is thought to dominate wet and dry mechanisms for acid deposition to such ecosystems (Lovett and Kinsman 1990) and also may be an important pathway for nutrient inputs (Weathers and Likens 1997). In otherwise arid regions, occult precipitation can account for a significant fraction of the water input to cloud forests and other affected vegetation (Schemenauer *et al.* 1988).

Attempts to quantify the effects of occult deposition have focused largely on measuring or modelling the magnitude of the water flux to the surface. Ionic chemical

* Corresponding author: Department of Biology, University of Antwerp (UIA), Universiteitsplein 1, B-2610 Wilrijk, Belgium.

fluxes could then be determined as the product of this quantity and the concentration of the chemical species found in the cloud water (Unsworth and Wilshaw 1989).

Models of droplet deposition to vegetation have been developed (Lovett 1984) and applied extensively (e.g. Miller *et al.* 1993; Pahl *et al.* 1994; Elias *et al.* 1995) but have yet to be evaluated against credible measurements. Many of the models rely on a proposed analogy between droplet deposition and 'deposition of momentum' (Chamberlain 1967; Slinn 1982). This assumption is examined here and found to be wanting in complex terrain where occult processes most frequently occur. Simpler models based on droplet impaction efficiencies (Langmuir 1961) are physically robust but require accurate information on within-canopy structure, wind speeds and size-dependent droplet number concentrations.

Measurements of accumulated uptake of deposited cloud water by turf sections (Fowler *et al.* 1990) or tree stands (Mueller and Imhoff 1989) beg the issue of 'representativeness', a particularly important consideration in complex terrain. Such methods also neglect the issues of canopy storage and evaporation. Micrometeorological methods are preferable in that area averaging over a surface 'footprint' is implicit (Schuepp *et al.* 1990). As is evidenced in results presented here and elsewhere (Gallagher *et al.* 1992b), direct application of the flux-gradient or K-theory approach is not appropriate for non-conservative scalars such as cloud water (Duyzer and Fowler 1994; Kowalski 1996). Relevant, physical processes which are not modelled by such a parametrization include phase change and gravitational settling (sedimentation).

Lewellen (1985) compared time-scales for turbulent eddies with the cloud-droplet relaxation time (the time required for a droplet to equilibrate inertially with the air due to drag only). The analysis showed that even a water droplet with a 50 μm diameter (much larger than the depositing cloud droplets of interest here) takes just thousandths of a second to equilibrate its motion with the airstream (i.e. to reach a Stokes equilibrium). Cloud droplets were found to diffuse just like a gaseous species; the droplets follow the eddies except when within 1 cm of surface elements. This meant that the effects of droplet trajectories crossing air streamlines could be neglected, and the eddy correlation (EC) technique could be applied to make direct measurements of cloud-water fluxes over forests.

Eddy correlation has been applied to the droplet deposition problem frequently in the last decade (Beswick *et al.* 1991; Gallagher *et al.* 1992b; Vong and Kowalski 1995; Vermeulen *et al.* 1997) and surface uptake has been estimated to be much smaller than predictions from modelling. Such direct measurements of liquid water (LW) fluxes also have revealed deposition of large cloud droplets occurring concurrently with transport of smaller droplets *away* from the depositing surface (e.g. Gallagher *et al.* 1992a,b). Vong and Kowalski (1995) employed the relative standard deviation in the cloud water concentration to isolate periods of 'steady cloud'. This data stratification was found to be more appropriate for studying deposition than for other processes which drive LW variability (e.g. entrainment) but it did not eliminate the upward flux of small droplets, which these authors attributed to the effects of phase change.

The scalar quantity analysed in micrometeorological studies of cloud-water deposition is the mass of cloud LW per unit air volume, or liquid water content (LWC, denoted as L in equations). Like most other studies, the measurements described here were made over sloping terrain where LWC has a source during the lifting of saturated air. For a non-conservative quantity such as LWC, an atmospheric source would lead one to expect the flux to *increase* (become more upward) with height above the ground (Businger 1986; Stull 1988; Kraus 1993; Kramm and Dlugi 1994; Duyzer and Fowler 1994). This invalidates the traditional assumption of a 'constant flux layer' and complicates

the determination of a surface flux from micrometeorological measurements. For flow over hills, there are other factors which can contribute to vertical changes in fluxes even of conservative scalars (Raupach *et al.* 1992).

On hill or mountain sides, characterization of surface stress is complicated by pressure gradients which effect 'mountain drag' on synoptic flow (Smith 1978). If the model relating droplet deposition to momentum transfer (Slinn 1982) is to be of practical use, it should be applicable in complex terrain where cloud-water deposition occurs most frequently and where fluxes of droplets and momentum are affected by different processes, including some not specifically related to surface transfer.

This paper presents concurrent measurements of vertical cloud-water and momentum fluxes at two heights and two horizontal locations above a forest canopy on the Pacific coast of North America. Vertical differences in the LW fluxes are large compared with measurement uncertainties which were determined from collocated measurements (Kowalski *et al.* 1997). Divergence of the LW flux is interpreted via the budget equation for LWC. Accounting for the vertical divergence of the turbulent cloud-water flux is found to be critical to the estimation of surface uptake in orographic cloud.

2. MEASUREMENTS

The measurements were taken during the third field campaign of the Cloud and Aerosol Chemistry Experiment (CACHE-3) which was conducted in late summer 1994 at the Cheeka Peak atmospheric observation station (CPO). The station is on the crest of a forested ridge on the Olympic Peninsula of Washington state ($48^{\circ}18' \text{ N}$, $124^{\circ}37' \text{ W}$); the ridge runs parallel to the Pacific coast at an elevation of 460 m and is approximately 3 km from the beach. For detailed topographic information see Vong and Kowalski (1995) and Kowalski (1996). The site frequently is engulfed in stratiform marine cloud. Aerosol, cloud, and rainwater chemistry in this region are characteristic of the remote marine atmosphere (Vong *et al.* 1988; Vong *et al.* 1997).

Turbulence and microphysical instruments were deployed to measure LWC and LW fluxes at three stations on two towers at the ridge summit. The two towers were separated by a distance of 28 m along a line transverse to the typical WSW winds during cloud events. The 'Walk' tower had one EC station with a sonic anemometer (ATI model SWS-211-3K) and a forward-scattering spectrometer probe (PMS FSSP-100-ER) 10 m above ground level (a.g.l.); the 'Flux' tower supported both a 10 and a 15 m station, each with a sonic anemometer and a particulate-volume monitor (GSI PVM-100). Each EC station also had a platinum resistance temperature probe (PRT) collocated with the sonic anemometer. These instruments and the data collection are described in detail by Kowalski *et al.* (1997).

In addition to the EC stations, two intervening towers supported profile measurements at 2.5 m intervals up to 15 m. Mean winds were measured with propeller-vane anemometers on the 'Prop' tower; temperature was measured with hygrothermometers on the 'Psys' tower. Mean values given in section 4 are from the most reliable level (7.5 m a.g.l.).

Canopy structure, which showed little variation in the typical upwind sector, was characterized along a 240° transect beginning at the Prop tower. Ten contiguous plots of 10 m^2 were demarcated in succession. The 202 trees (excluding saplings) were dominated by Pacific silver fir (72%), with some Western hemlock (26%) and a few Western red cedars. Typical canopy height was estimated to be 6.8 m. Leaf area index (LAI) measurements (Chason *et al.* 1991) averaged 7.0 (or 9.0 when including the

understorey of ericaceous shrubs) for this temperate rain forest. The terrain slope, measured with a clinometer, averaged 15.1° .

Instruments were deployed at a 'remote site' to measure below-cloud meteorological conditions upwind on the slope of Cheeka Peak at 200 m elevation. A data logger (Campbell Scientific Inc. model HMP35C) recorded five-minute means of temperature and relative humidity (RH). Vertical soundings (temperature and RH) from Quillayute, some 40 km to the south, were used to characterize the marine boundary layer.

3. ANALYSES

These analyses consider flux measurements which address the issue of spatial separation. Twenty-one cloud events (labelled A–U) spanned nineteen different calendar days from 15 August to 24 September 1994 and comprised over 400 half-hours with in-cloud measurements. Ensemble statistics have been compiled over these events and examined for relationships between LW fluxes and factors which ought to control them. Certain analyses excluded outlier data from some events due to large droplet sizes (for which the PVMs are less reliable; Kowalski *et al.* 1997), unusual flow conditions (section 4c) and saturated conditions at the below-cloud site. Three events were selected for presentation of time evolution and flow characteristics: two for reasons of cloud duration and data quality (I and D), and one for its unusual flow conditions (B).

(a) Statistical

Scalar fluxes were computed from covariances using 30 min Reynolds averaging. In the case of the FSSP data, covariances were calculated using size-dependent number concentrations as the scalars. These were multiplied by droplet volume to obtain size-dependent droplet fluxes, and integrated over the range of droplet sizes to determine the LW flux. Spikes in the sonic-anemometer outputs were identified via the method of Højstrup (1993), and the data were further screened for consistency in the winds as described by Kowalski *et al.* (1997). The relative standard deviation in LWC (σ_L/\bar{L} , defined for the 10 m station on the Flux tower) was used to identify steady-cloud periods, most appropriate for the determination of surface uptake in these EC measurements (Vong and Kowalski 1995; Kowalski *et al.* 1997). With these criteria satisfied, 129 periods were available with flux measurements at 10 and 15 m on the Flux tower; 107 periods were available with horizontally separated, 10 m fluxes; and 91 periods had good flux measurements at all three stations. Data which did not pass the screening criteria introduce gaps in the time series presented in section 4.

Eddy correlation studies in sloping topography require coordinate rotation in order to evaluate the surface-normal rather than true vertical flux. Kowalski *et al.* (1997) showed that the estimated surface-normal cloud-water flux is not sensitive to the precise method for determining the angle of rotation. Fluxes and, in particular, differences in fluxes from different stations were found to be insensitive to the use of rectilinear or streamline coordinate systems. This is consistent with predictions from scale analysis: the 'extra terms' introduced when using streamline coordinates (Kaimal and Finnigan 1994) scale as the flux divided by the radius of hill curvature. Since this scale is much smaller than the measured change in flux with height, these terms may be safely neglected. The results also showed no sensitivity to the time-averaging scale used to determine the rotation angles, whether half-hour or long-term ensemble averaging (over several weeks of in-cloud measurements) were used. At CPO, this may be unique to cloud-water fluxes since they occur in neutral conditions and rarely during weak winds; the effects of mesoscale circulations on EC turbulent fluxes (Sun *et al.* 1996)

are thus minimized. The 'local-mean' coordinate system is used here, with half-hour-mean streamlines defining the coordinate axes for each measurement location. In the remainder of this text, the distinction between surface-normal and vertical will be dropped.

Non-stationarity complicates the interpretation of EC results, particularly in complex terrain. McMillen (1988) suggested detrending each time series with a recursive, digital approximation to a running-mean filter and computing covariances with deviations from this running mean. Using this method, Vong and Kowalski (1995) found that fluxes of heat and LW during cloud events at CPO were insensitive to the filter time constant over a range of 50 to 10 000 s; the filtered fluxes were indistinguishable from the 30 min Reynolds flux. Momentum fluxes, on the other hand, depended strongly on the filter time constant.

Similar analysis of CACHE-3 data confirmed that momentum fluxes (but neither heat nor LW fluxes) depended upon the filtering operation. This means that correlations exist between u' and w' (streamwise and vertical perturbation velocity components) on scales larger than the eddies which transport droplets and heat. Such correlations suggest the presence of mesoscale motions associated with fluctuating pressure gradients in the hill vicinity. These mesoscale motions may modulate the turbulent fluxes of heat and droplets, but they are spectrally distinct from the eddies in terms of scalar transport. For the results presented here, all fluxes are computed from Reynolds averaging except momentum fluxes, which are computed using McMillen's method with a 100 s time constant. The filtering operation is applied to pre-rotated wind components (rotations based on half-hour means). This calculation purposefully filters out the so-called Leonard fluxes (Leonard 1974), a fact which may be important and is discussed later. The stress was computed from the product of deviations for the streamwise and surface-normal velocity components only (i.e. neglecting the $v'w'$ term).

(b) Physical

Sedimentation fluxes (F_{sed}) were calculated using the droplet-size-dependent gravitational settling velocity (defined negative-downward) specified as

$$v_{g,i} = -\rho_l g \frac{D_i^2}{18\mu} \quad (1)$$

where ρ_l is the density of liquid water, D_i is the volume-weighted mean droplet diameter for FSSP size interval i , and μ is the dynamic air viscosity, calculated as a weak function of temperature (Montgomery 1947). The sedimentation flux for any size interval i was taken as the product of the settling velocity for that interval and the interval-averaged LWC (L_i). The total sedimentation flux is thus the sum of the interval fluxes over all droplet sizes,

$$F_{\text{sed}} = \sum_{i=1}^{15} v_{g,i} L_i. \quad (2)$$

Roughness characteristics of the canopy were modelled based on physical measurements from the forest transect. The zero plane displacement (d) and the roughness length (z_0) were estimated using canopy height (h) and LAI via the methods described by Raupach (1992, 1994). The calculated displacement height of 4.2 m is in reasonable agreement with the choice of $d \sim 2h/3$ used by other investigators of cloud-water deposition to conifers (Beswick *et al.* 1991; Gallagher *et al.* 1992b; Pahl *et al.* 1994). The

roughness length was estimated to be 16.5 cm. This may seem a small estimate for a 7 m canopy. However, the tree density was quite high (ca. 2000 trees per hectare) and the canopy was closed even at such a young age. Thus, it is not unreasonable that this temperate rain forest exhibits less roughness than other conifer stands of similar height.

The remote-site temperature and RH were used to determine the height of cloud base on Cheeka Peak. An assumption of conserved water-vapour mixing ratio during sub-saturated ascent was combined with Poisson's equation to relate cloud-base temperature to the below-cloud thermodynamic conditions using the Newton–Raphson method (Press *et al.* 1986). Cloud-base height was then calculated using the remote-site temperature and elevation and the dry adiabatic lapse rate.

Advection of liquid water along the hillside was estimated from data as the product of the wind speed and the ratio of LWC to distance. This involved a combination of measurements and assumptions. Winds measured at the site were parallel to the upwind surface (Kowalski 1996; Kowalski *et al.* 1997). Since streamline curvature did not have a dominant effect on advection, wind speeds measured by the sonic anemometers at the summit were assumed to be representative of the winds along the slope upwind. The change in LWC was taken as the difference between the LWC measured at the summit and that at cloud base (zero). Rather than estimating the streamwise distance from cloud base to CPO, a substitution was used based on quantities which were estimable from measurements. Assuming a constant slope during ascent from cloud base, the ratio of wind speed to distance was assumed to be the same for streamwise and true vertical coordinates. Effectively, the streamwise distance to cloud base was estimated from available information regarding differences in altitude, such that

$$\bar{u} \frac{\partial \bar{L}}{\partial x} = \left(\bar{w} \frac{\partial \bar{L}}{\partial z} \right)_{\text{unrotated}}. \quad (3)$$

This estimate of advection reflects bulk processes operating on the slope of the hill, prior to any influence of the hill summit. It does not account for any streamwise variation in advection which would be due to the variation of surface sink strength (since droplets grow during ascent and larger droplets deposit more efficiently than smaller ones). It may be taken as a crude estimate, since some of the above assumptions cannot be verified. The motivation for this approach is discussed in section 5.

In-cloud, adiabatic liquid-water production (the source term) was calculated using the CPO air temperature, $\bar{w}_{\text{unrotated}}$ as in eq. (3), and a saturated adiabatic parcel model with an assumption of constant supersaturation during ascent.

4. RESULTS

Thick cloud characterized CACHE-3; for 312 half-hour periods with $\text{LWC} > 0.05 \text{ g m}^{-3}$, both the mean and median values of the 10 m LWC were 0.38 g m^{-3} and the maximum was 0.95 g m^{-3} . During steady cloud, the vertical gradient in LWC showed a consistent relationship with 11% more LWC at 15 m than at 10 m (Figure 1). Excluding outliers with very large droplet volume mean diameters (VMDs), 105 periods had slope = 1.11 ± 0.01 , $R^2 = 0.99$, and intercept = 0.001 g m^{-3} .

The turbulent LW fluxes exhibited no clear relationship with any thermodynamic or kinematic properties of the flow (e.g. \bar{u} , u_* , \bar{L} , \bar{T}). Most notably, counter-gradient fluxes were far from rare. In the following subsection, Figs. 2–7 show the time evolution of LWC, σ_L/\bar{L} , and LW fluxes (both turbulent and gravitational), plus representative

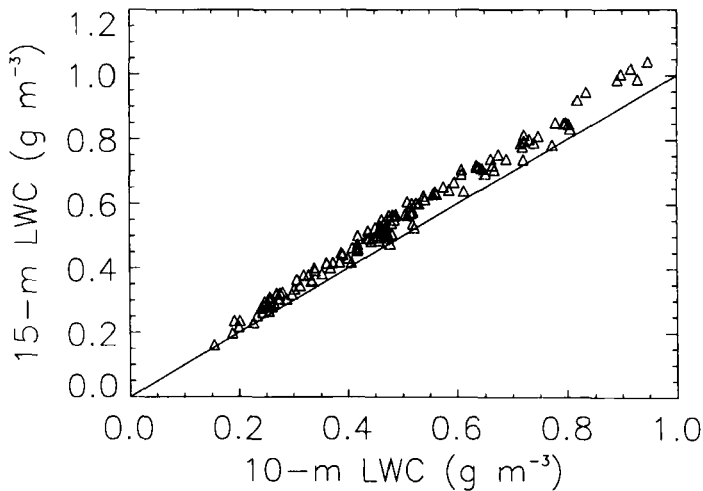


Figure 1. The gradient in liquid-water content (LWC) represented as a regression of the 15 m LWC versus the 10 m LWC for steady cloud. The 1:1 line is included for reference.

wind profiles for the three selected cloud events. For each event presented, the event-averaged (during steady cloud), size-dependent droplet deposition velocity ($v_d(d)$), the mean-scaled flux for each FSSP droplet size interval) is described. Local time (Pacific Daylight) lags UTC by eight hours.

(a) Selected Cloud Events

At 1800 h on 28 August, the site received a light rain shower from a cloud layer well above the site. The 1700 h sounding showed a cloud layer from about 750 m to 2500 m, with another thin cloud layer aloft. Apparently, the lower cloud layer descended onto the site and a cloud event began around 0100 h on 29 August (event I). No precipitation fell during this event. Wind speeds were light and steady at 2 m s^{-1} and the temperature was 12.2°C . The event was marked by two periods of steady cloud separated by an interval with more variability from 0400 to 0500 h (Fig. 2) and ended by 0930 h, after which the cloud layer broke into scattered cumulus.

The droplet VMD slowly increased from 13 to $15 \mu\text{m}$ through the event, with a slight decrease around 0430 h. During steady cloud, the two 10 m LW fluxes showed excellent agreement at ca. $-10 \text{ mg m}^{-2}\text{s}^{-1}$ (downward); the 15 m flux was near zero. During the variable cloud interval, all LW fluxes were more upward by ca. $20 \text{ mg m}^{-2}\text{s}^{-1}$ with excellent agreement in the two 10 m fluxes. Notably, the vertical flux divergence (10 m flux more downward than the 15 m flux) persisted with near constant magnitude while individual fluxes changed dramatically. Upward transport ($v_d(d) \sim 1 \text{ cm s}^{-1}$) of droplets with diameters less than $7 \mu\text{m}$ accompanied downward transport ($v_d(d) \sim -2 \text{ cm s}^{-1}$) of larger droplets. This event exhibited a low-level jet with a maximum in the wind profile at 12.5 m (Fig. 3).

On 13 August cloud arrived or formed just after dark following a clear sunset (event D). This event was typified by a LWC of 0.6 g m^{-3} , wind speeds of $3 - 4 \text{ m s}^{-1}$ and a steady temperature of 11.8°C . Steady cloud in the night gave way to more variable cloud on the morning of 14 August. The sounding at 0500 h on the 14th showed a saturated layer from the surface up to 800 m, capped by an inversion. No precipitation fell during

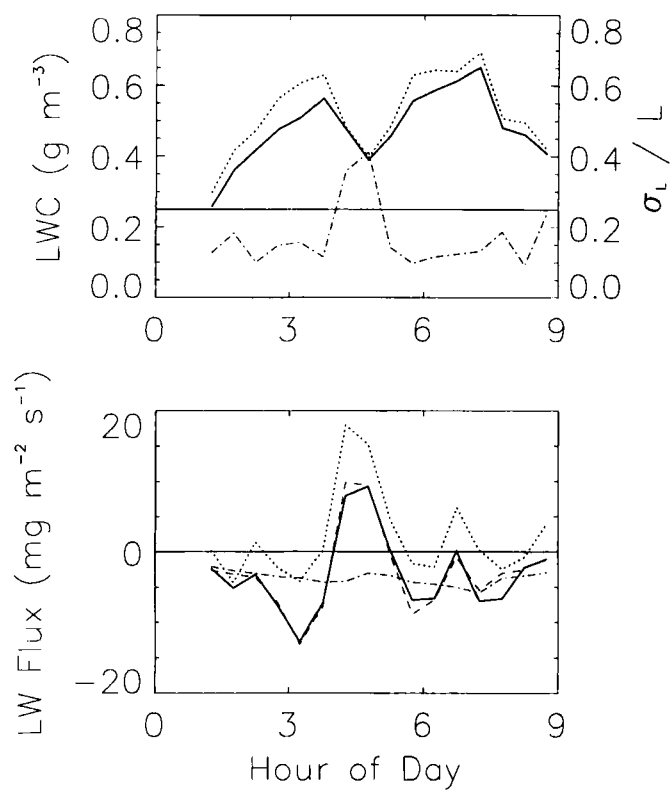


Figure 2. Time evolution of the cloud event on 29 August. Top panel shows liquid-water content (LWC) and the steady-cloud criterion (with threshold value of 0.25 indicated). Data are from the Flux tower (see text): 10 m LWC—heavy, solid line, 15 m LWC—dotted line, and σ_L / \bar{L} —dash-dotted line. Bottom panel shows LW fluxes from two towers: 10 m Flux tower, turbulent—heavy, solid line, 15 m Flux tower, turbulent—dotted line, 10 m Walk tower (see text), turbulent—dashed line and Sedimentation—dash-dot line.

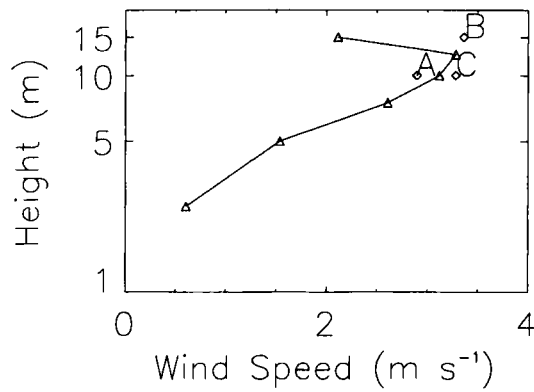


Figure 3. Wind profile for the half-hour period beginning at 0700 h on 29 August. Triangles denote the propeller-anemometer profile. Diamonds represent the sonic-anemometer mean winds. Lettered symbols for the sonic-anemometers are as follows: A is the 10 m station on the Flux tower (see text); B is the 15 m station; C is the 10 m station on the Walk tower (see text).

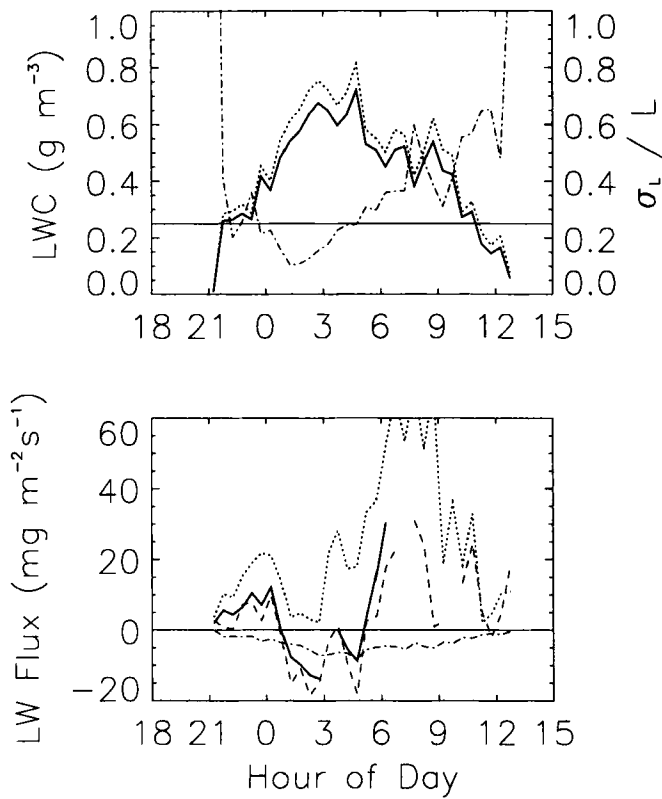


Figure 4. As Fig. 2 for 13 and 14 August.

this cloud event. The droplet VMD slowly increased from 12 to 15 μm during the steady portion of the event, with downward LW fluxes of the order of $-10 \text{ mg m}^{-2}\text{s}^{-1}$ at 10 m a.g.l. (good agreement between the two 10 m stations) and smaller upward fluxes at 15 m (Fig. 4). Again, the flux divergence was much more consistent than the individual fluxes. A low-level jet appeared in the wind profile (Fig. 5). Upward transport ($v_d(d) \sim 2 \text{ cm s}^{-1}$) of droplets with diameters less than 7 μm occurred simultaneously with downward transport ($v_d(d) \sim -2 \text{ cm s}^{-1}$) of larger droplets.

On the late afternoon of 11 August (prior to event B), with clear skies aloft, a marine stratus layer moved onshore, enveloped the remote site and reached CPO around 1700 h. The 1700 h sounding showed a moist, nearly saturated layer below an inversion at 650 m. Twelve hours later, a sounding revealed a saturated layer from the surface up to 550 m, capped by an inversion. Thick, steady cloud persisted from 2200 h until 0800 h on the 12 August (Fig. 6), with 5 m s^{-1} winds and a temperature of 10.0°C . The cloud event was without precipitation until 0600 h, when light drizzle began. The 10 m LWC during this event was over 0.8 g m^{-3} for most of the night.

The droplet VMD was typically 15 μm until early morning, when it increased and peaked near 19 μm just before dawn. Since the event had large droplet sizes and LWCs, the sedimentation flux was often of the order of $10 \text{ mg m}^{-2}\text{s}^{-1}$. During much of the steady portion of the event, LW fluxes were downward with a magnitude of about $-10 \text{ mg m}^{-2}\text{s}^{-1}$. Here, upward transport ($v_d(d) \sim 3 \text{ cm s}^{-1}$) of droplets

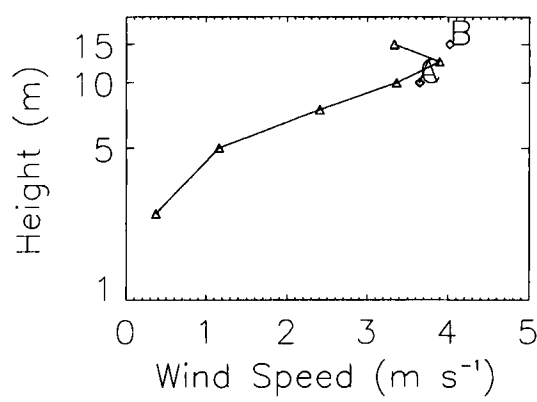


Figure 5. As Fig. 3 for the half-hour period beginning at 0430 h on 14 August.

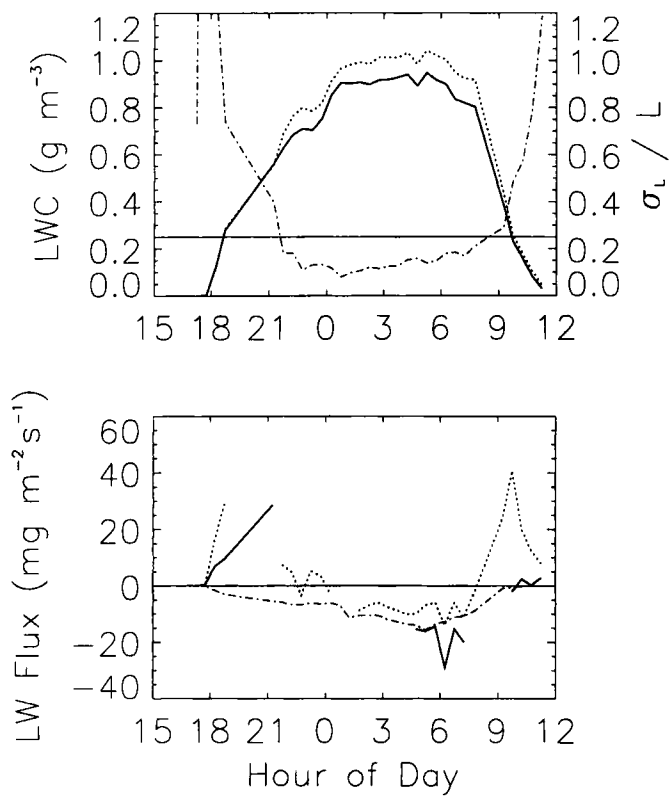


Figure 6. As Fig. 2 for 11 and 12 August. No turbulent fluxes from the Walk tower (see text) are presented (poor data quality).

with diameters smaller than $10\text{ }\mu\text{m}$ occurred at the same time as downward transport ($v_d(d) \sim -2\text{ cm s}^{-1}$) of larger droplets. The low-level jet (Fig. 7) was manifest on the Flux tower (10 m sonic wind speed exceeding the 15 m sonic wind speed) and appeared at a lower level on the Prop tower than other cloud events.

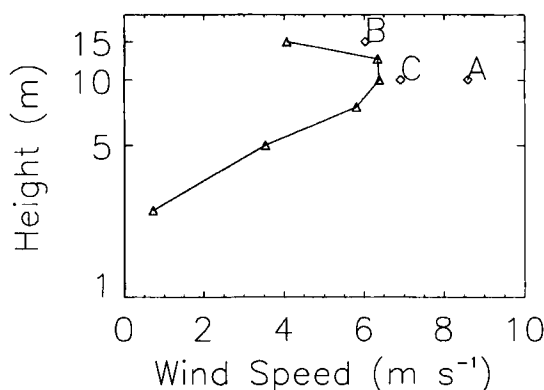


Figure 7. As Fig. 3 for the half-hour period beginning at midnight on 12 August.

(b) *LW fluxes and variances*

During steady cloud ($\sigma_L/\bar{L} < 0.25$), the turbulent LW fluxes at 10 m were downward at ca. $-10 \text{ mg m}^{-2} \text{ s}^{-1}$. Droplet size-dependent flux information from the FSSP revealed that small droplets, bearing a negligible fraction of the LWC, were transported upwards, while both larger droplets and cloud water in general were subject to downward transport. Two stations with 28 m lateral separation showed good agreement. The sedimentation flux was roughly half as large as the 10 m turbulent flux.

The 10 m turbulent LW flux was more downward than the 15 m flux by ca. $10 \text{ mg m}^{-2} \text{ s}^{-1}$, corresponding to a flux divergence. The surface flux is estimated to be more downward yet (section 5). Unlike other features of the turbulent LW fluxes, this divergence consistently occurred during both steady and more variable ($\sigma_L/\bar{L} > 0.25$) periods of cloud. The mean difference between 10 and 15 m fluxes during steady cloud was $8.9 \text{ mg m}^{-2} \text{ s}^{-1}$ and was significant at 99.95% confidence (relative to uncertainties determined by Kowalski *et al.* (1997)) and often exceeded the magnitude of either of the individual fluxes. Of the 129 steady-cloud periods with good data from both stations on the Flux tower, 19 exhibited upward fluxes at both stations, 55 had upward fluxes at 15 m and downward fluxes at 10 m, and 55 had downward fluxes at both stations.

The divergence of turbulent LW fluxes appears to have been confined to the vertical direction. Horizontal, turbulent LW fluxes were seen alternately to diverge and converge (i.e. no consistent sign in $\partial \overline{u'L'}/\partial x$ or $\partial \overline{v'L'}/\partial y$). The divergence averaged near zero and was rarely significant relative to the measurement error of the FSSP for horizontal fluxes (Kowalski *et al.* 1997).

The importance of analyzing LW fluxes during steady cloud is highlighted by the fact that sources of LW variability exist both at the surface and aloft; both sinks and sources of the scalar represent sources of scalar variance. Cloud-top entrainment represents a sink for LWC aloft (note that downward transport of dry air is equivalent to upward transport of cloud water). This is particularly evident in the relationship between the 10 m LW flux and the gradient in LW variance (Fig. 8).

When there is more LW variance at 15 m than at 10 m (positive variance gradient), cloud-top entrainment processes appear to be important and the 10 m flux is more upward. When entrainment is less important, generation of LW variance at the surface (due to deposition) dominates (negative variance gradient) and the flux is downward. This relationship suggests yet another steady-cloud criterion to minimize the influence

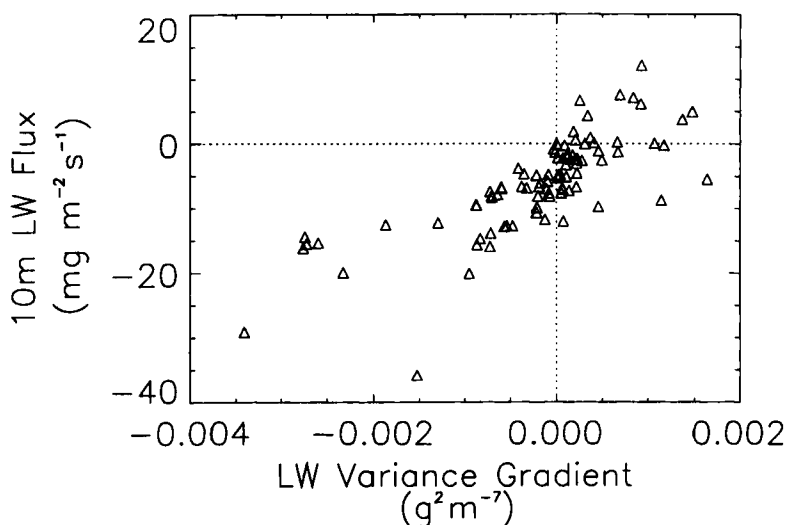


Figure 8. The 10 m liquid-water (LW) flux from the Flux tower (see text) versus the gradient in LW variance (positive for $L_{15} > L_{10}$ (see text)) for 129 half-hour steady-cloud intervals.

of entrainment processes on flux measurements which attempt to describe deposition. If entrainment were never a factor, one would expect the vertical gradient in LW variance always to be negative since the only source of variability would be due to deposition at the surface.

(c) Momentum

Figures 3, 5, and 7 present wind profiles which exhibit a reversal in the wind shear with height, termed a low-level jet. Interchange of instruments confirmed that this was not a measurement error, and it is believed to be a real aspect of CPO wind profiles during most cloud episodes. The height of the jet changed both with time and horizontal position since it was not always detected on both the Flux and Prop towers.

Eighty seven percent of all the half-hour wind profiles during steady-cloud conditions had the maximum wind speed (location of the jet) at 12.5 m on the Prop tower, 6% had the jet at 10 m, and 6% had monotonically increasing wind speed with height (no evidence of a jet). Event B was the only instance where the jet was at or below 10 m on the Prop tower and could be detected on the Flux tower.

Momentum fluxes during steady cloud are shown in Fig. 9. Excluding event B (outliers labelled in Fig. 9), these data showed excellent agreement between the 10 and 15 m stations on the Flux tower ($R^2 = 0.95$, slope = 1.06 ± 0.02 , negligible intercept for 123 half-hour intervals) with no consistent divergence or convergence in the momentum flux. While the momentum fluxes from the two stations agree, they are not always consistent with absorption of momentum at the surface; the momentum flux is sometimes upward at both stations. Unlike the droplet case, there was no relationship between the gradient of variance (turbulence kinetic energy) and the sign of the 10 m flux.

5. DISCUSSION

The gradient in LWC was the most consistent feature of these near-surface measurements in orographic cloud, with the 15 m LWC exceeding the 10 m LWC consistently

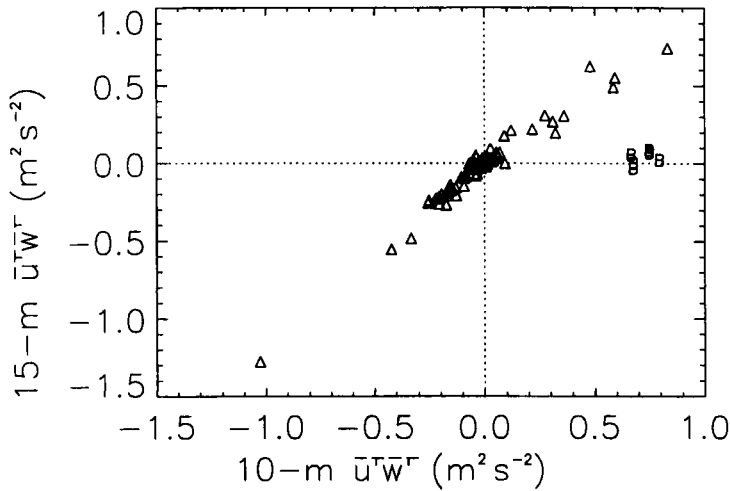


Figure 9. The 15 m momentum flux versus the 10 m momentum flux (both from the Flux tower (see text)) for 129 half-hour steady-cloud intervals.

by 11%. While the sign of the LW gradient was constant, the LW fluxes were highly variable in sign and generally showed no relationship to the gradient.

(a) LW Fluxes

Unlike previous investigations of cloud-water deposition, CACHE-3 saw LWCs and especially droplet sizes so large that droplet sedimentation fluxes sometimes were of the same magnitude as the turbulent LW fluxes. For marine cloud, the sedimentation flux cannot be ignored as a means of transporting droplets to a depositing surface. The mean sedimentation flux for steady cloud during CACHE-3 was $-4.7 \text{ mg m}^{-2} \text{ s}^{-1}$. For ground-based measurements of cloud in more continental environments, droplets are typically smaller and more numerous, such that the sedimentation flux would probably be small in comparison with turbulent fluxes.

The existence of steady cloud (absence of substantial entrainment) appears to be the most important factor in predicting the behaviour of the turbulent LW fluxes at a given height. The influence of cloud-top entrainment could lead to a divergence in the cloud-water flux. Typical cloud-top heights, derived from soundings launched 40 km from the CPO site, were between 600 and 700 m (Kowalski 1996), not far above the 460 m site elevation. Analysis of nocturnal data in steady cloud showed that upward cloud-water fluxes coincided with radiative cooling (net radiation measurements), also suggesting proximity to cloud top. However, for steady cloud, most often the LW fluxes were downward. The LW variance gradient results presented in Fig. 8 suggest that, while entrainment may sometimes dominate the LW variability near the surface and lead to upward fluxes, it is not usually important during steady cloud.

The strikingly consistent feature of the LW turbulent fluxes was the vertical divergence which persisted across steady and more variable periods of cloud (e.g. Fig. 2). Individual turbulent fluxes at 10 or 15 m a.g.l. otherwise showed little consistency. However, the agreement between the 10 m fluxes with nearly 30 m of horizontal separation suggests that these point observations of cloud-water fluxes can be taken as representative of the 10 m flux along the ridge top. The droplet size dependence of the flux

(measured by the FSSP) was consistent in that upward fluxes of small droplets always accompanied downward fluxes of the larger droplets during steady cloud.

The divergence of the turbulent LW flux is both significant relative to measurement uncertainties and important given that the sign of the 10 and 15 m fluxes often disagreed. Considering only measurements from 15 m, where LW fluxes were usually upwards, the common assumption of a constant flux layer might lead an investigator to conclude that the forest was most often a mean source for cloud LWC. This clearly is not the case. Furthermore, for counter-gradient fluxes such as those usually measured at 15 m (and sometimes at 10 m), the deposition velocity (v_d) is poorly defined since it does not always describe a deposition process. The flux normalized by the mean LWC is better termed a scale velocity, representing various processes of which deposition is but one.

A number of possibilities have been considered for factors which may account for the divergence of LW fluxes. For example, Raupach *et al.* (1992) pointed out that hilltop fluxes of even conservative scalars can vary with height due to the effects of flow over hills. Not all of these influences have been assessed by direct measurement. While some are believed (by inference) not to dominate, there is insufficient evidence to reject any of them as contributing to the divergence of liquid-water fluxes on the hilltop. Nevertheless, the LW budget equation presented below, while not explicitly accounting for these effects, reasonably predicts the flux divergence as a result of the source and advection terms which are important on the hillside.

Convergence/divergence of streamlines can be important near hill summits. The scale of the flow over the ridge at CPO is such that the motion can be considered incompressible (Mahrt 1986). Still, vertical streamline convergence corresponds to vertical advection of LWC since it implies a mean motion in the surface-normal direction (which has a strong LW gradient). At CPO, the 'attack angles' for the 10 and 15 m measurement stations were found to be in agreement (Kowalski *et al.* 1997), indicating parallel flow. Furthermore, non-parallel streamlines would depend upon wind speed and slope for the approaching wind direction; if important for the LW budget, they ought to have an effect on the LW gradient. Conversely, the gradient of LWC (shown above) did not vary over a broad range of wind speeds and directions.

Another factor which might contribute to diverging fluxes is the curvature of streamlines at the hilltop. Since a flux is a rate of mass exchange per unit area, a change in the stream-surface area across which droplets are transported may lead to a change in the flux with height. Considering the flow's increasing radius of curvature with height, an upward flux would diverge due to this effect. However, a downward flux would converge for the same reason, yet the measured flux divergence was independent of the direction of the individual fluxes. Furthermore, this effect can be neglected based on scale analysis, as explained in section 3a.

Vertical stress gradients could also affect the fluxes of LW, through spatial changes in the eddy diffusivity. Section 4 showed momentum fluxes at 10 and 15 m with the same magnitude and sign, but with a significant convergence during event B. The LW flux divergence for event B was similar to all other events, a fact which argues against the vertical stress gradient being responsible for the diverging LW fluxes. The LW flux divergence also could be affected by adjustments in the turbulent eddies to changes associated with flow over the hilltop.

The upwind footprint (Schuepp *et al.* 1990) varies with the measurement height such that the 15 m flux measurement represents surface-atmosphere interaction further upwind than for the 10 m measurement station. The footprint for the 15 m flux thus extends lower in the cloud, where the droplets are smaller and less efficiently captured by the needles. For downward fluxes at both stations, this is a plausible explanation of

the flux divergence. Kowalski (1996) estimated that the difference in footprints for these two measurement heights is less than 100 m in the streamwise direction, or less than 20 m in altitude along the hill slope.

The context for interpreting the LW flux divergence is the turbulent budget equation for the scalar LWC (Businger 1986)

$$\frac{\partial \bar{L}}{\partial t} + \frac{\partial \bar{u} \bar{L}}{\partial x} = -\frac{\partial \bar{u}_i' \bar{L}'}{\partial x_i} + D \frac{\partial^2 \bar{L}}{\partial x^2} - \frac{\partial \bar{v}_g \bar{L}}{\partial z} + \bar{S}_L. \quad (4)$$

In this equation, u and x are defined in the streamwise direction, while u_i and x_i are generalized. Local changes and advection (on the left-hand side) are balanced by the convergence of three types of fluxes (turbulent, molecular and sedimentation) and the source for cloud water in the ambient air. The budget equation describes possible fates for cloud water in a layer parallel to the surface and bounded by the two measurement heights. This equation is written in the rotated coordinate system (x -axis is streamwise) and can be simplified by considering turbulent fluxes in the surface-normal (z) direction only. A scale analysis has allowed further simplification by neglecting the measured storage term, computed sedimentation fluxes (and their convergence) and molecular fluxes (Kowalski 1996), leading to an equation of the form

$$\bar{S}_L = \frac{\partial \bar{w}' \bar{L}'}{\partial z} + \bar{u} \frac{\partial \bar{L}}{\partial x}. \quad (5)$$

This simplified equation describes a steady-state balance between the source term and the sum of the flux divergence and advection. Every term in (5) is positive as written. Production of LW at the site acts to increase the LWC but is balanced by the effects of advective fluxes which act to supply LW-depleted air (advection) and transport droplets out of the layer (the turbulent flux divergence).

The simplified budget equation is tested against direct measurements in Fig. 10, which plots the sum of the flux divergence and advection against the source term. The data suggest that the budget equation (5) contains the most important terms and is not far from closure. This is of particular interest considering all of the effects (above) which have not been explicitly included. The mean magnitudes (for 54 steady-cloud periods) of the various terms in (5) are $4.0 \text{ mg m}^{-3} \text{ s}^{-1}$ for the source term, $1.5 \text{ mg m}^{-3} \text{ s}^{-1}$ for the flux divergence, and $2.2 \text{ mg m}^{-3} \text{ s}^{-1}$ for advection. The picture is biased somewhat by the inclusion of only those events which had no cloud at the remote site (and therefore did have an advection estimate). Including more extensive steady-cloud data (where no advection estimate is available), the source term is twice as large as the flux divergence in the mean (3.6 compared to $1.8 \text{ mg m}^{-3} \text{ s}^{-1}$).

While assessing the degree of closure for the LW budget equation, it is important to keep in mind the complicating effects (described above) which lead to uncertainties, particularly in the advection term. The flux divergence is well characterized based on the uncertainties in LW fluxes (Kowalski *et al.* 1997). However, the reasons for the flux divergence are not yet well understood, particularly given the complexity of turbulent flow over a ridge top such as CPO. The advection term represents a somewhat crude estimate since many of the assumptions used in its computation are not verifiable. The spatial scale over which it has been measured is not clearly the appropriate scale to match the turbulent fluxes. The wind speeds measured at the summit are not likely to be representative of those along the hill slope, and the validity of assuming a constant wind angle is unknown. Nevertheless, the budget equation described is consistent with the observations of diverging fluxes, and with the fact that condensation adds LWC to the

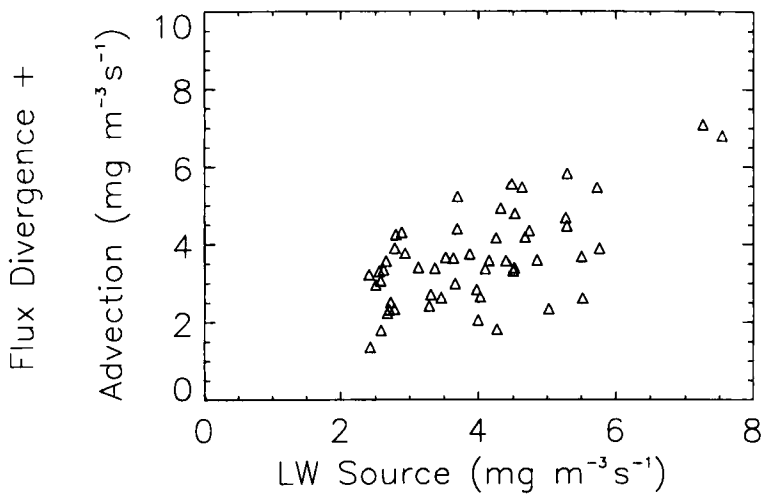


Figure 10. Testing closure of the budget equation: the sum of liquid-water (LW) advection and the LW flux divergence versus the LW source term for all data which passed the screening criteria *and* had reliable data from the remote site. See text for further explanation.

cloud as a consequence of ascent. Finally, inclusion of the advection term improves closure of the budget since the source term is typically twice as large as either the advection or the turbulent flux divergence terms.

It remains to use the measured change in the flux with height to estimate the LW flux at the canopy surface. Instead of a constant flux with height, some form must be assumed for the vertical change of the flux. Here, for simplicity, it is assumed that the surface flux can be predicted as a linear combination of the fluxes measured at 10 and 15 m. The validity of such an assumption is unknown. Two possibilities are considered: a simple linear extrapolation of the measured fluxes (Mann and Lenschow 1994), and another estimate based upon a dependence on the mean wind speed. The motivation for the latter is described presently.

In the simplified budget equation (5), both advection and the source term depend directly on the mean wind speed. Furthermore, the vertical variation in these terms is dominated by the vertical variation in the mean wind speed. If the budget is truly closed, this would mean that the entire equation, and therefore the flux divergence, also must vary vertically with the mean wind speed. The same need not be true for each of the individual fluxes. Analysis of wind profile data from the Prop tower showed that, the jet notwithstanding, the mean wind speed averaged from the surface to 10 m could be related to the mean wind speed in the layer between 10 and 15 m in a linear model as

$$\int_{10\text{m}}^{15\text{m}} \overline{u}(z) \, dz = 1.6 \int_{d+z_0}^{10\text{m}} \overline{u}(z) \, dz, \tag{6}$$

describing 86% of the variance in these two integrated quantities for 469 half-hour cloud intervals (both steady and more variable cloud). This relationship is probably dependent upon hill slope, surface roughness and the unperturbed velocity profile upwind (Hunt *et al.* 1988); it may not be appropriate for other hilltop sites.

The flux divergence between 10 m and the surface is predicted based on the flux divergence measured between 10 and 15 m. The flux at the surface, defined as $d = 4.2$ m (consistent with Beswick *et al.* 1991), is thus estimated as a linear combination of the

TABLE 1. COMPARISON OF 10 M LW FLUXES FOR VARIOUS STUDIES

Study	Hours	\overline{L} (g m ⁻³)	\overline{u} (m s ⁻¹)	v_d (cm s ⁻¹)	$\overline{w'L'}_{10m}$ (mg m ⁻² s ⁻¹)
Beswick <i>et al.</i> (1991)	7	0.05–0.35	4–10	0–4	0–8
Gallagher <i>et al.</i> (1992a)	NA	<0.2	15	ca. 10	8–10
Vong and Kowalski (1995)	11.5	<0.4	4–10	1–3	2–10
Vermeulen <i>et al.</i> (1997)	36	<0.4	1–4	0–10	1–6
Present Study	64.5	0.2–1.0	2–10	0–8	0–15

measured fluxes

$$\overline{w'L'}_{sfc} = \overline{w'L'}_{10m} + \alpha(\overline{w'L'}_{10m} - \overline{w'L'}_{15m}). \tag{7}$$

If simple linear extrapolation is used, then $\alpha = 0.86$ according to the ratio of layer thicknesses. However, normalizing each term in the budget by the mean wind speed in the appropriate layer, facilitated by (6), results in a smaller estimate for surface uptake ($\alpha = 0.73$).

Equation (7) assumes that the divergence in LW fluxes between 10 and 15 m is useful for predicting the divergence between 10 m and the surface. The applicability of such a formulation elsewhere is likely to depend on the same features which determine the structure of flow over the hill, including hill dimensions, flow stability (i.e. the Froude number), surface roughness, and other factors determining the formation of a wake in the lee of the hill. A rich body of literature exists on turbulent flow over hills, most of which is based on the work of Hunt *et al.* (1988).

Applying (7) to the turbulent LW fluxes at CPO, and taking $\alpha = 0.73$, results in a prediction for the turbulent flux to the surface which is quite large compared to the 10 m flux. The 10 m flux typically underestimates this surface flux by 20–50%, sometimes with the wrong sign. The mean turbulent flux to the surface of $-13.8 \text{ mg m}^{-2}\text{s}^{-1}$ during steady cloud was nearly twice the mean flux measured at 10 m ($-7.2 \text{ mg m}^{-2}\text{s}^{-1}$).

To put these estimates into context, Table 1 compares direct measurements of LW fluxes measured at 10 m from several studies. Most of the measurements were made over coniferous canopies on maritime or coastal hills at several hundred metres of elevation. The exception is the 50 m elevation (maritime plain) for Vermeulen *et al.* (1997). In the table, the LW flux values given are magnitudes; only downward fluxes are considered.

For a variety of wind speeds and LWCs, the eddy correlation studies of occult deposition have produced near-surface fluxes in the range of 0 to $15 \text{ mg m}^{-2}\text{s}^{-1}$ and deposition velocities ranging from 0 to 10 cm s^{-1} . If the flux divergence is similar for hillside studies other than CACHE-3, then these fluxes may underestimate deposition by a factor of two. Models of occult deposition, using assumed deposition velocities based on the momentum analogy, have predicted fluxes one and two orders of magnitude greater (c.f. Miller *et al.* 1993; Pahl *et al.* 1994; Walmsley *et al.* 1996).

Total canopy uptake of LW (i.e. the *surface* flux) was estimated as the sum of the turbulent LW flux from (7) and the sedimentation flux, which was presumed constant with height near the surface. Surface LW fluxes during steady cloud averaged $-18.6 \text{ mg m}^{-2}\text{s}^{-1}$, and typically fell in a range from -5 to $-50 \text{ mg m}^{-2}\text{s}^{-1}$. If a new deposition velocity (v_d) is defined as the ratio of this surface flux to the LWC at a reference height (10 m), then it may be of use for comparisons with models of droplet deposition. This v_d , usually between -1 and -3 cm s^{-1} but often ranging to (downward) magnitudes exceeding 10 cm s^{-1} , showed poor correlation ($R^2 < 0.1$) with the mean wind speed and the friction velocity. The reasons for this are described below in the discussion on momentum fluxes. Furthermore, it is important to recognise that the

concept of a deposition velocity is quite dependent upon the assumption of a constant flux with height. For fluxes which change with height, the mean-scaled flux (or droplet velocity scale) also changes with height and is not representative of surface deposition processes. The 'deposition velocity' is therefore inappropriate for description of cloud droplet deposition in complex terrain.

(b) Momentum

Most of the wind profiles measured at CPO exhibited a low-level jet on the 15 m Prop tower. The jet height varied from event to event but was rarely low enough to be seen on the Flux tower, just 20 m away. Hill-top jets have been observed (Bradley 1980) and have appeared in wind tunnel studies (Teunissen *et al.* 1987) and model simulations (Deaves 1976) of flow over hills. Attempts to describe the height of the jet in terms of hill dimensions and roughness characteristics have yielded inconsistent results, possibly because the height varies with rarely measured features such as the height of the overlying inversion (Carruthers and Choularton 1982).

Momentum fluxes have been calculated using a detrending procedure designed to filter out large-scale motions which represent non-stationarity in near-surface turbulence. These Leonard stress terms have been neglected in the budget equation for momentum (below), a fact which leads to further uncertainties in the computed surface stress. However, without such a procedure, the fluxes are very difficult to interpret since they can be in virtually any direction. The momentum budget equation can be expressed as the budget for streamwise winds,

$$\frac{\partial \bar{u}}{\partial t} + \frac{1}{2} \frac{\partial \bar{u} \bar{u}}{\partial x} = - \frac{\partial \overline{u'_j u'_i}}{\partial x_j} + D \frac{\partial^2 \bar{u}}{\partial x_j^2} - \frac{1}{\rho} \frac{\partial p_N}{\partial x}, \quad (8)$$

which describes a balance between local time change and advection on the left-hand side with turbulent and molecular diffusion and the effects of non-hydrostatic pressure perturbations on the right-hand side. For the neutral flow conditions prevailing during cloud events, the effects of buoyancy are neglected. Coriolis terms have also been excluded from this analysis. The budget includes advection and the effects of local pressure gradients, neither of which have been measured in this campaign; both can be important in complex terrain. The characterization of surface fluxes on a hillside is probably more difficult for momentum than for cloud water.

Chamberlain (1967) proposed, and the Slinn (1982) model assumed, that deposition of momentum and particles or droplets should be similar, assuming that the quantities in question are transported by the same eddies. This proposed similarity has been investigated extensively for cloud-water deposition (always using a filtering operation for flux computation, as described in section 3). It has been found perhaps to be valid for flat surfaces (Vermeulen *et al.* 1997); however, it has yielded poor results for applications in complex terrain where cloud-water deposition is more prevalent (Beswick *et al.* 1991; Vong and Kowalski 1995).

Measurements of mean profiles and fluxes at CPO have revealed numerous dissimilarities (relevant to deposition) between droplets (or LWC) and momentum. While the gradient in LWC was consistently positive, mean wind profiles typically showed opposing gradients above and below the jet. Time-scales for eddy transport of the two quantities are different; droplet transport appears to be accomplished exclusively by small-scale turbulence whereas transport of momentum may extend to the mesoscale since momentum fluxes depended strongly on the high-pass filtering time-scale (particularly relative to the 30 min Reynolds stress). Droplet fluxes consistently were divergent due

to advection and the condensational source term; momentum fluxes were non-divergent except when the jet intervened between the two measurement heights, and then a flux convergence was measured (Fig. 9). Neither the individual LW fluxes nor the LW flux divergence appeared to be influenced by the position of the jet. Finally, LW fluxes were usually downward during steady cloud and were related to the variance gradient; the sign of the momentum fluxes was not consistent during steady cloud and no relationship was noted between the flux and the variance gradient.

The lack of similarity between droplets and momentum is not surprising when considering the different processes affecting fluxes of these two quantities in complex terrain. LWC has a mean source due to lifting up the hillside. Changes in momentum fluxes due to pressure gradients are likely to vary spatially like the position of the jet. Further, the physical mechanisms by which the two quantities are transferred to the surface are quite different. Efficient surfaces for droplet impaction have minimal surface area (a spider web has excellent dimensions for impaction). Conversely, momentum is absorbed at the canopy via forces of form and frictional drag. Each of these is proportional to surface area. Finally, momentum transport on hillsides may not even be accomplished primarily by turbulence (Finnigan 1985).

6. CONCLUSIONS

Cloud-water deposition is an important pathway for the delivery of water and solute to some forest ecosystems. Even for estimation of chemical inputs, the greatest uncertainty in assessing the magnitude of deposition is in the estimation of the water flux. Eddy correlation is the best available means of determining this flux, but requires particular attention due to the non-conservative nature of the scalar LWC, and the fact that the process typically occurs in complex terrain. Sedimentation is important when mean droplet sizes are large (VMD exceeding ca. 15 μm).

Spatially separated measurements of vertical turbulent LW fluxes at a site on the Pacific coast of North America showed little variation in the horizontal direction (transverse to winds) and a significant divergence in the vertical. The 10 m flux was consistently more downward than the 15 m flux. The vertical flux divergence was related to both a LW source (from condensation) and LW advection. Other factors may play roles but are not specifically assessed here. A simple method was developed to predict the surface flux based on the measured change in the flux with height. The estimated surface flux was often twice as large as the 10 m flux.

The results of this investigation present new challenges for the modelling of cloud-water deposition. One-dimensional modelling using the aerodynamic resistance (inverse of the deposition velocity; Monteith (1965)) incompletely describes cloud-water deposition in orographic cloud unless an atmospheric source term is included. Characterization of the structure and deposition of momentum on a hillside is fraught with difficulties including the effects of pressure gradients (which are rarely measured) and any hill-top jet. Comparison of profiles and fluxes of momentum and cloud water have revealed numerous dissimilarities. Since there is no direct, physical relationship between droplet deposition and the deposition of momentum, there is no advantage in modelling cloud water deposition in complex terrain based on momentum fluxes.

Cloud-water deposition is a particular challenge for eddy correlation due to its tendency to occur in complex terrain, the non-conservative nature of the scalar, and the intermittent effects of cloud-top entrainment. Estimating vertical fluxes from deposition velocities or a vertical gradient in scalar concentration and wind speed are of questionable validity. Issues requiring future study include (a) the degree to which these

results apply to other sites (LW flux measurements at multiple heights), (b) the droplet size dependence of the vertical change in the flux, (c) a more precise estimate of the advection term to close the budget equation for cloud water and (d) the comparison of (new) occult deposition models with measurements of surface uptake such as those presented here.

ACKNOWLEDGEMENTS

The authors extend gratitude to Hermann Gerber for the loan of an instrument. Thanks go also to Dave Covert, Pit Anthoni, Fred Brechtel, Jeff Shykula and the entire team from the National Center for Atmospheric Research (NCAR) Atmospheric Surface Turbulent Exchange Research facility for much help in planning and executing CACHE. Lee Klinger of NCAR made measurements of canopy structure and LAI that were important to the determination of surface roughness. Mike Unsworth, John Finnigan, and Larry Mahrt helped significantly with the interpretation of results. This work was supported by National Science Foundation (USA) grant ATM9118316 (Atmospheric Chemistry desk).

REFERENCES

- | | | |
|---|-------|---|
| Beswick, K. M., Hargreaves, K.,
Gallagher, M. W.,
Choularton, T. W. and
Fowler, D. | 1991 | Size-resolved measurements of cloud droplet deposition velocity to a forest canopy using an eddy correlation technique. <i>Q. J. R. Meteorol. Soc.</i> , 117 , 623–645 |
| Bradley, E. F. | 1980 | An experimental study of the profiles of wind speed, shearing stress and turbulence at the crest of a large hill. <i>Q. J. R. Meteorol. Soc.</i> , 106 , 101–123 |
| Businger, J. A. | 1986 | Evaluation of the accuracy with which dry deposition can be measured with current micro meteorological techniques. <i>J. Clim. Appl. Meteorol.</i> , 25 , 1100–1124 |
| Carruthers, D. J. and
Choularton, T. W. | 1982 | Airflow over hills of moderate slope. Pp 83–103 in <i>Atmospheric processes over complex terrain</i> . Ed. W. Blumen. American Meteorol. Soc., Boston, USA |
| Chamberlain, A. C. | 1967 | Transport of <i>Lycopodium</i> spores and other small particles to rough surfaces. <i>Proc. R. Soc. London</i> , 296A , 45–70 |
| Chason, J. W., Baldocchi, D. D. and
Huston, M. A. | 1991 | A comparison of direct and indirect methods for estimating forest canopy leaf area. <i>Agric. Forest Meteorol.</i> , 57 , 107–128 |
| Deaves, D. M. | 1976 | Wind over hills: a numerical approach. <i>J. Ind. Aerodyn.</i> , 1 , 371–391 |
| Duyzer, J. and Fowler, D. | 1994 | Modelling land atmosphere exchange of gaseous oxides of nitrogen in Europe. <i>Tellus</i> , 46B , 353–372 |
| Elias, V., Tesar, M. and Buchtele, J. | 1995 | Occult precipitation: sampling, chemical analysis and process modelling in the Sumava Mts. (Czech Republic) and in the Taunus Mts. (Germany). <i>J. Hydrol.</i> , 166 , 409–420 |
| Finnigan, J. J. | 1985 | Turbulent transport in flexible plant canopies. Pp 353–372 in <i>The Forest–Atmosphere Interaction</i> . Eds. B. A. Hutchinson and B. B. Hicks. Reidel Publishing Co., Dordrecht, the Netherlands |
| Fowler, D., Morse, A. P.,
Gallagher, M. W. and
Choularton, T. W. | 1990 | Measurements of cloud water deposition on vegetation using a lysimeter and a flux gradient technique. <i>Tellus</i> , 42B , 285–293 |
| Gallager, M. W., Beswick, K. and
Choularton, T. W. | 1992a | Measurements and modelling of cloudwater deposition to a snow-covered canopy. <i>Atmos. Environ.</i> , 26A , 2893–2903 |
| Gallager, M. W., Beswick, K.,
Choularton, T. W., Coe, H.,
Fowler, D. and Hargreaves, K. | 1992b | Measurements and modelling of cloudwater deposition to moorland and forests. <i>Environ. Pollution</i> , 75 , 97–107 |
| Højstrup, J. | 1993 | A statistical data screening procedure. <i>Meas. Sci. Technol.</i> , 4 , 153–157 |
| Hunt, J. C. R., Leibovich, S. and
Richards, K. J. | 1988 | Turbulent shear flows over low hills <i>Q. J. R. Meteorol. Soc.</i> , 114 , 1435–1470 |

- Kaimal, J. C. and Finnigan, J. J. 1994 *Atmospheric boundary layer flows*. Oxford University Press, New York.
- Kowalski, A. S. 1996 'Occult cloudwater deposition to a forest in complex terrain: measurement and interpretation'. Ph.D. thesis, Oregon State University
- Kowalski, A. S., Anthoni, P. M., Vong, R. J., Delany, A. C., and Maclean, G. D. 1997 Deployment and evaluation of a system for ground-based measurement of cloud liquid water turbulent fluxes. *J. Atmos. Oceanic. Technol.*, **14**, (3), 468–479
- Kramm, G. and Dlugi, R. 1994 Modelling of the vertical fluxes of nitric acid, ammonia, and ammonium nitrate. *J. Atmos. Chem.*, **18**, 319–357
- Kraus, H. 1993 Surface-layer fog considered using a modified Monin–Obukhov theory. *Boundary-Layer Meteorol.*, **66**, 219–235
- Langmuir, I. 1961 Mathematical investigation of water droplet trajectories. Pp 335–393 in *The collected works of Irving Langmuir*. Eds. C. G. Suits and H. E. Way. Pergamon Press, New York, USA
- Leonard, A. 1974 Energy cascade in large-eddy simulations of turbulent flow fields. *Adv. Geophys.*, **18A**, 237–248
- Lewellen, W. S. 1985 Modeling turbulent exchange in forest canopies. Pp. 481–499 in *The forest–atmosphere interaction* Eds. B. A. Hutchinson and B. B. Hicks. Reidel Publishing Co., Dordrecht, the Netherlands
- Lovett, G. M. 1984 Rates and mechanisms of cloud water deposition to a subalpine balsam fir forest. *Atmos. Environ.*, **18**, (2), 361–371
- Lovett, G. M. and Kinsman, J. D. 1990 Atmospheric pollutant deposition to high-elevation ecosystems. *Atmos. Environ.*, **24A**, (11), 767–786
- McMillen, R. T. 1988 An eddy correlation technique with extended applicability to non-simple terrain. *Boundary-Layer Meteorol.*, **43**, 231–245
- Mahrt, L. 1986 On the shallow motion approximations. *J. Atmos. Sci.*, **43**, (10), 1036–1044
- Mann, J. and Lenschow, D. H. 1994 Errors in airborne flux measurements. *J. Geophys. Res.*, **99**, (D7), 14519–14526
- Miller, E. K., Friedland, A. J., Arons, E. A., Mohnen, V. A., Battles, J. J., Panek, J. A., Kadlecsek, J. and Johnson, A. H. 1993 Atmospheric deposition to forests along an elevational gradient at Whiteface Mountain, NY, USA. *Atmos. Environ.*, **27A**, 2121–2136
- Monteith, J. L. 1965 Evaporation and environment. *Symp. Soc. Exp. Biol.*, **19**, 205–234
- Montgomery, R. B. 1947 Viscosity and thermal conductivity of air and diffusivity of water vapor in air. *J. Meteorol.*, **4**, (4), 193–196
- Mueller, S. F. and Imhoff, R. E. 1989 Inferring cloud deposition to a forest canopy using a passive cloudwater collector. *Geophys. Res. Lett.*, **16**, (7), 683–686
- NAPAP 1993 National Acidic Precipitation Assessment Program, 1992 Report to Congress. NAPAP Office of the Director, Washington DC, USA
- Pahl, S., Winkler, P., Schneider, T., Arends, B., Schell, D., Maser, R. and Wobrock, W. 1994 Deposition of trace substances via cloud interception on a coniferous forest at Kleiner Feldberg. *J. Atmos. Chem.*, **19**, 231–252
- Press, W. H., Teukolsky, S. A., Vetterling, W. T. and Flannery, B. P. 1986 *Numerical recipes in FORTRAN: the art of scientific computing*. Cambridge University Press, Cambridge, UK
- Raupach, M. R. 1992 Drag and drag partition on rough surfaces. *Boundary-Layer Meteorol.*, **60**, 375–395
- 1994 Simplified expressions for vegetation roughness length and zero-plane displacement as functions of canopy height and area index. *Boundary-Layer Meteorol.*, **71**, 211–216
- Raupach, M. R., Weng, W. S., Carruthers, D. J. and Hunt, J. C. R. 1992 Temperature and humidity fields and fluxes over low hills. *Q. J. R. Meteorol. Soc.*, **118**, 191–225
- Schemenauer, R. S., Fuenzalida, H. and Cereceda, P. 1988 A neglected water resource: the Camanchaca of South America. *Bull. Am. Meteorol. Soc.*, **69**, 138–147
- Schuepp, P. H., Leclerc, M. Y., MacPherson, J. I. and Desjardins, R. L. 1990 Footprint prediction of scalar fluxes from analytical solutions of the diffusion equation. *Boundary-Layer Meteorol.*, **50**, 355–373
- Shuttleworth, W. J. 1976 A one-dimensional theoretical description of the vegetation-atmosphere interaction. *Boundary-Layer Meteorol.*, **10**, 273–302

- Slinn, W. G. N. 1982 Predictions for particle deposition to vegetative canopies. *Atmos. Environ.*, **16**, 1785–1794
- Smith, R. B. 1978 A measurement of mountain drag. *J. Atmos. Sci.*, **35**, 1644–1654
- Stull, R. B. 1988 *An introduction to boundary layer meteorology*. Kluwer Academic Publishers, Dordrecht, the Netherlands
- Sun, J., Howell, J. F., Esbensen, S. K., Mahrt, L., Greb, C. M., Grossman, R. and LeMone, M. A. 1996 Scale dependence of air–sea fluxes over the western equatorial Pacific. *J. Atmos. Sci.*, **53**, (21), 2997–3012
- Teunissen, H. W., Shokr, M. E., Bowen, A. J., Wood, C. J. and Green, D. W. R. 1987 The Askervein Hill project: wind-tunnel simulations at three length scales. *Boundary-Layer Meteorol.*, **40**, 1–29
- Unsworth, M. H. and Wilshaw, J. C. 1989 Wet, occult and dry deposition of pollutants on forests. *Agric. Forest Meteorol.*, **47**, 221–238
- Vermeulen, A. T., Wyers, G. P., Romer, F. G., Van Leeuwen, N. F. M., Draaijers, G. P. J. and Erisman, J. W. 1997 Fog deposition on a coniferous forest in the Netherlands. *Atmos. Environ.*, **31**, (3), 375–386
- Vong, R. J., Baker, B. M., Brechtel, F. J., Collier, R. T., Harris, J. M., Kowalski, A. S., McDonald, N. C. and McInnes, L. M. 1997 Ionic and trace element composition of cloudwater collected on the Olympic peninsula of Washington state. *Atmos. Environ.*, **31**, (13), 1991–2001
- Vong, R. J., Hansson, H. B., Ross, H. B., Covert, D. S. and Charlson, R. J. 1988 Northeastern Pacific sub-micrometer aerosol and rainwater composition: a multivariate analysis. *J. Geophys. Res.*, **93**, (D2), 1625–1637
- Vong, R. J. and Kowalski, A. S. 1995 Eddy correlation measurements of size-dependent cloud droplet turbulent fluxes to complex terrain. *Tellus*, **47B**, 331–352
- Walmsley, J. L., Schemenauer, R. S. and Bridgman, H. A. 1996 A method for estimating the hydrologic input from fog in mountainous terrain. *J. Appl. Meteorol.*, **35**, 2237–2249
- Weathers, K. C. and Likens, G. E. 1997 Clouds in southern Chile: An important source of nitrogen to nitrogen-limited ecosystems? *Environ. Sci. Technol.*, **31**, 210–213
- Wyngaard, J. C. 1973 On surface-layer turbulence. Pp. 101–149 in *Workshop on Micrometeorology*. Ed. D. A. Haugen. American Meteorol. Soc., Boston, USA